J Radioanal Nucl Chem (2016) 307:69–77
DOI 10.1007/s10967-015-4135-0

Neutral $^{99m}Tc(CO)_3$ complexes of "clicked" nitroimidazoles for the detection of tumor hypoxia

Mohini Bhadwal[1] · Madhava B. Mallia[1] · Haladhar Dev Sarma[2] · Sharmila Banerjee[1]

Received: 25 November 2014 / Published online: 8 May 2015

Abstract In the present work, three neutral $^{99m}Tc(CO)_3$ complexes of nitroimidazole were synthesized and their potential to detect tumor hypoxia is evaluated in vivo. Triazole derivatives of 2-, 4- and 5-nitroimidazole were synthesized via 'click chemistry' route. The ligands synthesized were characterized and subsequently radiolabeled using $[^{99m}Tc(CO)_3(H_2O)_3]^+$ precursor complex to obtain corresponding neutral $^{99m}Tc(CO)_3$ complexes in >90 % radio chemical purity. The complexes were subsequently evaluated in Swiss mice bearing fibrosarcoma tumor and in vivo distribution observed was thoroughly analyzed. All complexes showed uptake in tumor, however, contrary to general expectations, the 5-nitroimidazole complex showed significantly higher tumor uptake ($p < 0.05$) at 30 min and 60 min p.i., compared to the 2-nitroimidazole counterpart. Though a conclusive explanation for this observation could not be obtained, present study underlined the significance of evaluating nitroimidazole radiotracers other than 2-nitroimidazole for detecting tissue hypoxia.

Keywords Hypoxia · Nitroimidazole · $[^{99m}Tc(CO)_3(H_2O)_3]^+$ precursor complex · Click-chemistry · Neutral complexes · Biodistribution

Electronic supplementary material The online version of this article (doi:10.1007/s10967-015-4135-0) contains supplementary material, which is available to authorized users.

✉ Sharmila Banerjee
sharmila@barc.gov.in

[1] Radiopharmaceuticals Chemistry Section, Bhabha Atomic Research Centre, Mumbai 400085, India

[2] Radiation Biology and Health Sciences Division, Bhabha Atomic Research Centre, Mumbai 400085, India

Introduction

The negative influence of hypoxia in the clinical management of cancer is well documented [1–9]. Information on hypoxic status of cancerous lesion can help in patient selection for hypoxia directed treatment and to bring appropriate alterations to treatment strategy for a better clinical outcome [1]. Nitroimidazoles which show selective accumulation in hypoxic cells are the most widely explored molecules for delineating hypoxic tumor cells from normoxic cells [10]. Several nitroimidazole radiopharmaceuticals based on PET as well as SPECT isotopes are reported [11–28]. Presently, [^{18}F]fluoromisonidazole ([^{18}F]FMISO), a 2-nitroimidazole-radiotracer, is the radiopharmaceutical of choice for clinical imaging of tumor hypoxia [29]. However, owing to optimal decay characteristics, easy availability and low cost of ^{99m}Tc, a nitroimidazole radiopharmaceutical based on this isotope may find wider applicability. Though, several ^{99m}Tc-labeled nitroimidazole radiopharmaceuticals are evaluated for detecting tumor hypoxia, ^{99m}Tc-BRU59-21 is, probably, the only complex that reached phase-I clinical trials [30]. Other complexes evaluated so far have not shown suitable pharmacokinetics for hypoxia detecting applications in a clinical setup. This aspect has provided the impetus for the development of new nitroimidazole radiopharmaceuticals labeled with ^{99m}Tc for targeting tumor hypoxia.

Introduction of unconventional ^{99m}Tc-cores, such as $[^{99m}TcN]^{+2}$ core and $[^{99m}Tc(CO)_3]^+$ core, for radiolabeling biomolecules have alleviated the problems associated with the usage of the conventional ^{99m}Tc-oxo or ^{99m}Tc-dioxo cores to a great extent. The $[^{99m}TcN]^{+2}$ core and $[^{99m}Tc(CO)_3]^+$ core are easy to prepare and stable over a wide range of pH conditions. The $[^{99m}Tc(CO)_3(H_2O)_3]^+$ precursor complex, introduced by Alberto et al., is

especially attractive for radiolabeling small bio-molecules and peptides. Three labile water molecules in $[^{99m}Tc(CO)_3(H_2O)_3]^+$ precursor complex permits radiolabeling with a suitable tridentate ligand resulting in the formation of a stable pseudo-octahedral complex [31].

In the present work, the concept of 'click chemistry' was employed to prepare triazole derivatives of three differently substituted nitroimidazoles viz. 2-, 4- and 5-nitroimidazole, for radiolabeling with $[^{99m}Tc(CO)_3]^+$ core [32–34]. Triazole ligands form neutral pseudo-octahedral complex with $[^{99m}Tc(CO)_3(H_2O)_3]^+$ precursor complex [32]. The three, differently substituted, neutral, nitroimidazole-triazole complexes prepared were subsequently evaluated in Swiss mice bearing fibrosarcoma tumor. The biodistribution results obtained are thoroughly analyzed and compared with clinically used hypoxia imaging agent [^{18}F]FMISO.

Experimental

Materials and methods

2-Nitroimidazole, 4-nitroimidazole, 1,3-dibromopropane, anhydrous potassium carbonate and L-propargyl glycine were procured from M/s. Fluka, Germany. Copper sulphate, sodium azide, ascorbic acid and sodium carbonate were purchased from S.D. Fine Chemicals, Mumbai, India. Flexible silica gel plates used for thin layer chromatography (TLC) were obtained from Bakerflex Chemical Company, Germany. The HPLC analyses were performed on a JASCO PU 2080 Plus dual pump HPLC system, Japan, with a JASCO 2075 Plus tunable absorption detector and a Gina Star radiometric detector system, using a C18 reversed phase HiQ Sil column (5 μm, 4 × 250 mm). All the solvents used for HPLC were degassed and filtered prior to use and were of HPLC grade. IR spectra of the synthesized compounds were recorded on JASCO-FT/IR-420 spectrometer, Japan. ^{1}H-NMR spectra were recorded using 300 MHz Bruker Avance II, spectrometer, Germany. Mass spectra were recorded on Varian 500 MS Ion Trap mass spectrometer, USA using electron spray ionization (ESI) in positive mode.

Synthesis

*Synthesis of 1-(3-bromopropyl)-2-nitro-1H-imidazole (**1**)*

Compound **1** was prepared from 2-nitroimidazole (0.11 g, 1 mmol) and 1,3-dibromopropane (0.59 g, 10 mmol) in presence of crushed anhydrous K_2CO_3 in acetonitrile (10 mL) [22]. The reaction mixture was stirred overnight at room temperature. Upon completion of the reaction (cf. TLC), solvent was removed under vacuum and the residue was dissolved in water (30 mL). The aqueous layer was extracted with chloroform (15 mL × 3). Combined organic layer was washed with brine and dried over anhydrous sodium sulphate. The dried organic layer was concentrated and purified by silica gel column chromatography to obtain compound **1** (0.19 g, 80 %). R_f (diethylether) = 0.22. IR (neat, cm^{-1}) 3121(m); 2918(w); 2853(w); 1545(s); 1406(s); 1044(s); 656(s). ^{1}H-NMR (δ ppm, $CDCl_3$) 2.41 (m, 2H, –CH_2C$\underline{H}_2CH_2$Br), 3.38 (t, 2H, –CH_2CH_2C$\underline{H}_2$Br), 4.63 (t, 2H, –C$\underline{H}_2CH_2CH_2$Br), 7.22 (s, 1H, 2-nitroimidazole-C5-H), 7.27 (s, 1H, 2-nitroimidazole-C4-H).

*Synthesis of 1-(3-bromopropyl)-4-nitro-1H-imidazole and 1-(3-bromopropyl)-5-nitro-1H-imidazole (**2** & **3**)*

Compounds **2** and **3** were prepared in a one-pot reaction between 4-nitroimidazole (0.5 g, 4.4 mmol) and 1,3-dibromopropane (2.6 g, 44 mmol) in presence of crushed anhydrous K_2CO_3 as base in acetonitrile (10 mL) [22]. The reaction mixture was kept stirring overnight at room temperature. Upon completion of the reaction (cf. TLC), the mixture was worked-up following a procedure similar to the one described for compound **1**. Compound **2** and **3** were separated by silica gel column chromatography using diethyl ether. Yield of compound **2** was 75 % (0.77 g) and that of compound **3** was 11 % (0.11 g).

Compound **2**: R_f (diethylether) = 0.3. IR (neat, cm^{-1}) 3121(m); 2918(w); 2853(w); 1545(s); 1406(s); 1044(s); 656(s). ^{1}H-NMR (δ ppm, $CDCl_3$) 2.36 (m, 2H, –CH_2-C$\underline{H}_2CH_2$Br), 3.36 (t, 2H, –CH_2CH_2C$\underline{H}_2$Br), 4.27 (t, 2H, –C$\underline{H}_2CH_2CH_2$Br), 7.52 (s, 1H, 4- nitroimidazole-C2-H), 7.84 (s, 1H, 4-nitroimidazole-C5-H).

Compound **3**: R_f (diethylether) = 0.4. IR (neat, cm^{-1}) 3114(w); 2969(w); 1529(s); 1371(s); 1121(s); 741(s); 650(w). ^{1}H-NMR (δ ppm, $CDCl_3$) 2.39 (m, 2H, –CH_2-C$\underline{H}_2CH_2$Br), 3.36 (t, 2H, –CH_2CH_2C$\underline{H}_2$Br), 4.59 (t, 2H, –C$\underline{H}_2CH_2CH_2$Br), 7.74 (s, 1H, 5-nitroimidazole-C2-H), 8.03 (s, 1H, 5-nitroimidazole-C4-H).

General procedure for synthesis of nitroimidazole azides

Bromide derivatives of different nitroimidazoles were converted into corresponding azides by reacting with NaN_3 in dimethylformamide [27]. Upon completion of the reaction the solvent was removed using rotary evaporator. The residue was dissolved in water (30 mL) and extracted with chloroform (15 mL × 3). Combined organic layer was washed with brine, concentrated and purified by silica gel column chromatography to obtain corresponding nitroimidazole azide.

*Synthesis of 1-(3-azidopropyl)-2-nitro-1H-imidazole (**4**)*

Compound **4** was prepared from compound **1** (0.15 g, 0.64 mmol) and NaN_3 (0.04 g, 0.64 mmol) following the general procedure described above. Yield 75 % (0.09 g). R_f (chloroform) = 0.28. IR (neat, cm^{-1}) 3114(m); 2936(w); 2873(w); 2099(s); 1537(s); 835(s). ^{1}H-NMR (δ ppm, $CDCl_3$) 2.12 (m, 2H, $–CH_2\underline{CH_2}CH_2N_3$), 3.38 (t, 2H, $–CH_2CH_2\underline{CH_2}N_3$), 4.51 (t, 2H, $–\underline{CH_2}CH_2CH_2N_3$), 7.14 (s, 1H, 2-nitroimidazole-C5-H), 7.15 (s, 1H, 2-nitroimidazole-C4-H).

*Synthesis of 1-(3-azidopropyl)-4-nitro-1H-imidazole (**5**)*

Compound **5** was prepared by reaction of compound **2** (0.5 g, 2.13 mmol) with NaN_3 (0.14 g, 2.13 mmol) following the general procedure described above. The yield of the reaction was 75 % (0.32 g). R_f (chloroform) = 0.21. IR (neat, cm^{-1}) 3126(m); 2921(w); 2099(s); 1541(s); 1126(s); 831(s). ^{1}H-NMR (δ ppm, $CDCl_3$) 2.09 (m, 2H, $–CH_2\underline{CH_2}CH_2N_3$), 3.38 (t, 2H, $–CH_2CH_2\underline{CH_2}N_3$), 4.16 (t, 2H, $–\underline{CH_2}CH_2CH_2N_3$), 7.49 (s, 1H, 4-nitroimidazole-C2-H), 7.83 (s, 1H, 4-nitroimidazole-C5-H).

*Synthesis of 1-(3-azidopropyl)-5-nitro-1H-imidazole (**6**)*

Compound **6** was prepared by reaction of compound **3** (0.05 g, 0.21 mmol) with NaN_3 (0.02 g, 0.21 mmol) following the general procedure stated above. The yield of the reaction was 60 % (0.03 g). R_f (chloroform) = 0.25. IR (neat, cm^{-1}) 3119(m); 2926(w); 2881(w); 2100(s); 1523(s); 1125(s); 824(s); 648(vs). ^{1}H-NMR (δ ppm, $CDCl_3$) 2.08 (m, 2H, $–CH_2\underline{CH_2}CH_2N_3$), 3.38 (t, 2H, $–CH_2CH_2\underline{CH_2}N_3$), 4.51 (t, 2H, $–\underline{CH_2}CH_2CH_2N_3$), 7.68 (s, 1H, 5-nitroimidazole-C2-H), 8.03 (s, 1H, 5-nitroimidazole-C4-H).

General procedure for synthesis of triazole from azide

Different terminal nitroimidazole azides were converted into corresponding triazoles via "click reaction" with L-propargyl glycine in presence of sodium ascorbate and copper sulphate in water [27]. The reaction mixture was kept stirring at room temperature for 36 h. It was subsequently washed with dichloromethane to remove excess nitroimidazole azide.

*Synthesis of 2-amino-3-(1-(3-(2-nitro-1H-imidazol-1-yl)propyl)-1H-1,2,3-triazol-4-yl)propanoic acid (**7**)*

Compound **4** (50 mg, 0.26 mmol), L-propargyl glycine (30 mg, 0.26 mmol), ascorbic acid (20 mg, 40 mol %) and $CuSO_4{\cdot}2H_2O$ (10 mg, 20 mol %) were dissolved in 3 mL of double distilled water. The reaction was carried out following general procedure stated above. Overall yield of **7** was 40 % (30 mg). IR (KBr, cm^{-1}) 3407(m); 2949(w); 1773(s); 1626(s); 1486(s); 1359(m); 1285(m); 1111(s); 832(s); 616(s). ESI-MS (*m/z*): $C_{11}H_5N_7O_4$ MS (ESI^+): 309.2$(M)^+$.

*Synthesis of 2-amino-3-(1-(3-(4-nitro-1H-imidazol-1-yl)propyl)-1H-1,2,3-triazol-4-yl)propanoic acid (**8**)*

Compound **5** (0.02 g, 0.10 mmol), L-propargyl glycine (0.08 g, 0.74 mmol), ascorbic acid (0.06 g, 40 mol %) and $CuSO_4{\cdot}2H_2O$ (0.04 g, 20 mol %) were dissolved in 3 mL of double distilled water. The reaction was carried out following general procedure stated above. Overall yield of **8** was 47 % (0.11 g). IR (KBr, cm^{-1}) 3426(m); 2956(w); 1640(s); 1486(m); 1404(m); 1290(s); 1219(m); 1124(s); 1060(s); 825(s). ESI-MS (*m/z*): $C_{11}H_5N_7O_4$ MS (ESI^+): 309.1 $(M)^+$.

*Synthesis of 2-amino-3-(1-(3-(5-nitro-1H-imidazol-1-yl)propyl)-1H-1,2,3-triazol-4-yl)propanoic acid (**9**)*

Compound **6** (0.12 g, 0.61 mmol) with L-propargyl glycine (0.07 g, 0.61 mmol), ascorbic acid (0.05 g, 40 mol %) and $CuSO_4{\cdot}2H_2O$ (0.03 g, 20 mol %) were dissolved in 3 mL of double distilled water. The reaction was carried out following general procedure stated above. Overall yield of **9** was 44 % (0.08 g). IR (KBr, cm^{-1}) 3439(m); 2924(m); 1735(s); 1633(s); 1398(v); 1305(m); 1226(m); 1131(s); 533(m); 616(s). ESI-MS (*m/z*): $C_{11}H_5N_7O_4$ MS (ESI^+): 309.1$(M)^+$.

*Preparation of 4-nitroimidazole-triazole-Re(CO)$_3$ complex (**13**)*

The rhenium analogue of 4-nitroimidazole-triazole-[^{99m}Tc(CO)$_3$] was prepared by refluxing a mixture of 4-nitroimidazole-triazole (0.17 g, 0.55 mmol) and bis(tetraethylammonium)-*fac*-tribromotricarbonylrhenate (0.42 g, 0.55 mmol) in 5 mL water for 15 h [27]. The compound bis(tetraethylammonium)-*fac*-tribromotricarbonylrhenate was prepared following a procedure reported by Alberto et al. [28]. After refluxing, reaction mixture was allowed to cool down and then filtered. The filtrate was evaporated under vacuum to yield the 4-nitroimidazole-triazole-Re(CO)$_3$ complex as tetraethylammonium salt (0.152 g, 48 %). ESI-MS (*m/z*): $C_{14}H_{14}N_7O_7Re$ MS (ESI^+): 601.8 $(M+Na)^+$.

Radiolabeling

Preparation of [^{99m}Tc(CO)$_3$(H$_2$O)$_3$]$^+$ precursor complex

The [^{99m}Tc(CO)$_3$(H$_2$O)$_3$]$^+$ precursor complex was prepared following the procedure reported by Alberto et al.

[35]. An aqueous solution of sodium borohydride (5.5 mg), sodium carbonate (4 mg) and sodium potassium tartrate (15 mg) in 0.5 mL double distilled water in a sealed 10 mL vial was purged with carbon monoxide gas for 5 min. To this solution freshly eluted $Na^{99m}TcO_4$ (1 mL, ~37 MBq) was added and the mixture was heated at 80 °C for 15 min. The reaction mixture was then cooled on an ice bath for 5 min. The pH of the reaction mixture was adjusted to 7 using 0.5 M phosphate buffer (pH 7.5): 1 M HCl (1:3 v/v) and subsequently characterized by HPLC.

*General procedure for the radiolabeling of nitroimidazole triazole derivatives (**7**, **8** & **9**) with $[^{99m}Tc(CO)_3(H_2O)_3]^+$ precursor to prepare $^{99m}Tc(CO)_3$ complexes of 2-, 4- and 5-nitroimidazoles (**10**, **11**, **12**)*

To 900 μL of 10^{-3} M solution of respective nitroimidazole triazole ligand in saline, 100 μL of freshly prepared $[^{99m}Tc(CO)_3(H_2O)_3]^+$ precursor complex was added and the radioactive solution incubated at 80 °C for 45 min. The solution was then cooled to room temperature and the complex obtained was characterized using HPLC.

Quality control

HPLC

The radiochemical purity (RCP) of $[^{99m}Tc(CO)_3(H_2O)_3]^+$ precursor complex as well as different nitroimidazole-$^{99m}Tc(CO)_3$ complexes (**10**–**12**) was assessed by HPLC with a C18 reversed phase column. About 15 μL of the test solution (~0.37 MBq) was injected into the column and elution was monitored by observing the radioactivity profile. Aqueous 0.05 M triethylammonium phosphate (TEAP) buffer, pH = 2.5 (Solvent A) and methanol (Solvent B) were used as the mobile phase. Both the solvents were filtered through 0.22 μ filter. The elution started with 100 % A from 0 to 6 min. At 6 min the eluent switched to 75 % A and 25 % B and at 9 min to 66 % A and 34 % B followed by a linear gradient 66 % A/34 % B to 100 % B from 9 to 20 min. Up to 30 min the eluent remained at 100 % B before switching back to the initial condition. Flow rate was maintained at 1 mL/min.

Determination of octanol–water partition coefficient (Log $P_{o/w}$)

The radiolabeled compound (0.1 mL) was mixed with double distilled water (0.9 mL) and *n*-octanol (1 mL) on a vortex mixer for about 3 min and then centrifuged at 3500 g for 5 min to effect clear separation of the two layers. The *n*-octanol layer (0.8 mL) was withdrawn and equal volume of fresh double distilled water was added. The mixture was vortexed and then centrifuged as described above. Equal aliquots of the two layers were withdrawn and measured for the radioactivity. The readings thus obtained were used to calculate the Log $P_{o/w}$ value of the complex.

In vitro serum stability and protein binding studies

About 50 μL of the labeled complex (**10**, **11** or **12**) was added to 0.45 mL of human serum and this solution was incubated at 37 °C. After 3 h, ethanol (0.5 mL) was added to this solution to precipitate serum proteins. The mixture was centrifuged and the supernatant was analyzed by HPLC to assess the stability of the complex in serum. The activity associated with protein pellet was determined in a well-type NaI(Tl) detector. The ratio of activity associated with the protein pellet to the activity initially added to serum gives a measure of activity bound to serum protein.

Biological studies

All procedures performed herein were in strict compliance with the national laws governing the conduct of animal experiments. Solid tumor was developed in Swiss mice by implantation of HSDM1C1 murine fibrosarcoma. About 10^6 cells in 100 μL volume were injected subcutaneously on the dorsum of each animal. The tumors were allowed to grow till they were approximately 10 mm in diameter after which the animals were used for the experiment. For the biodistribution studies, the radioactive preparation (~0.37 MBq per animal in 100 μL volume) was administered intravenously through the lateral tail vein. Individual sets of animals ($n = 5$) were utilized for studying the biodistribution at different time points (30, 60, and 180). At the end of the respective time periods, the animals were sacrificed and the relevant organs excised for measurement of retained activity. The organs were weighed and the activity associated with them was measured in a flat-bed type NaI(Tl) counter with suitable energy window for ^{99m}Tc. The activity retained in each organ/tissue was expressed as percentage injected dose per gram (%ID/g).

Statistical analysis

Statistical analysis of relevant data was performed by one-way analysis of variance (ANOVA). Confidence level of 95 % ($p < 0.05$) was taken for statistical significance.

Results and discussion

Appropriate terminal azides when 'clicked' with L-propargyl glycine form tridentate triazole ligands suitable for preparing neutral $^{99m}Tc(CO)_3$ complexes in high RCP

and in vivo stability. This strategy was adopted to convert 2-, 4- and 5-nitroimidazole azide derivatives into corresponding tridentate triazole ligands (**7–9**) as shown in Scheme 1. All intermediates were characterized by appropriate spectroscopic techniques. Mass spectrometric analysis confirmed the identity of target compounds **7–9**. Following the optimized protocol, the nitroimidazole triazole derivatives (**7–9**) were radiolabeled using freshly prepared $[^{99m}Tc(CO)_3(H_2O)_3]^+$ precursor complex (Scheme 2). The $[^{99m}Tc(CO)_3(H_2O)_3]^+$ precursor complex as well as the $^{99m}Tc(CO)_3$ complexes of 2-, 4-, and 5-nitroimidazole triazole (**10**, **11**, **12**) were analyzed by reversed phase HPLC following the gradient elution program described in the experimental section. The HPLC retention time observed for the three nitroimidazole-triazole-$^{99m}Tc(CO)_3$ complexes is summarized in Table 1. Typical HPLC profile of $[^{99m}Tc(CO)_3(H_2O)_3]^+$ precursor complex and one of the three nitroimidazole triazole complex (**12**) is shown in Fig. 1. The HPLC peak area measurements showed that RCP of all the complexes were >90 %. Lipophilicity (Log $P_{o/w}$) of the complexes was determined following a reported procedure (Table 1) [36]. Serum stability studies showed that all the complexes (**10–12**) were stable in human serum when incubated at 37 °C for 3 h. Serum protein binding studies of the complexes (**10–12**) showed that about 30–35 % activity was associated with the serum proteins upon incubation in the human serum at 37 °C for 3 h (Table 1). To obtain evidence for the structure of $^{99m}Tc(CO)_3$-complexes prepared at the tracer level, a 4-nitroimidazole triazole-$Re(CO)_3$ complex was prepared in macroscopic level. Matching HPLC elution profile of 4-nitroimidazole triazole-$Re(CO)_3$ complex and corresponding $^{99m}Tc(CO)_3$ complex prepared at the tracer level indicated the formation of structurally similar complexes (Table 1). A $(M+Na)^+$ ion peak at *m/z* 601.8 in the mass spectrum provided another confirmatory evidence for the formation of the expected 4-nitroimidazole triazole-$Re(CO)_3$ complex.

Biological evaluations of all the three nitroimidazole-triazole-$^{99m}Tc(CO)_3$ complexes (**10–12**) were carried out in Swiss mice bearing fibrosarcoma tumor. Though the hypoxic status of the fibrosarcoma tumor used for the present study was not determined, a systematic study by Markus et al. on a number of murine tumors, including a fibrosarcoma tumor, had shown that these tumors are hypoxic [37]. Additionally, biodistribution of [^{18}F]FMISO carried out earlier in the fibrosarcoma tumor model being used in the present study had shown significant tumor uptake which provided an indirect evidence for the hypoxic nature of the tumor [26].

Biodistribution of the complexes (**10–12**) was studied at three time points viz. 30 min, 1 and 3 h. Tumor uptake observed with the three nitroimidazole complexes is shown in Table 2. For comparison, tumor uptake observed with [^{18}F]FMISO is also shown in Table 2. Similar to our earlier observations, all the complexes showed relatively fast clearance from tumor between 30 min and 1 h post injection (p.i.), which could be attributed to the clearance of unbound nitroimidazole complex from the tumor. Slow clearance of tumor activity observed after 1 h p.i. is attributed to the hypoxia specific reduction and trapping of the radiotracer in tumor [26].

The effectiveness of a nitroimidazole complex to detect hypoxic tumor cells depend on factors such as its single electron reduction potential (SERP), ease with which the nitroimidazole complex enters the hypoxic cells and the

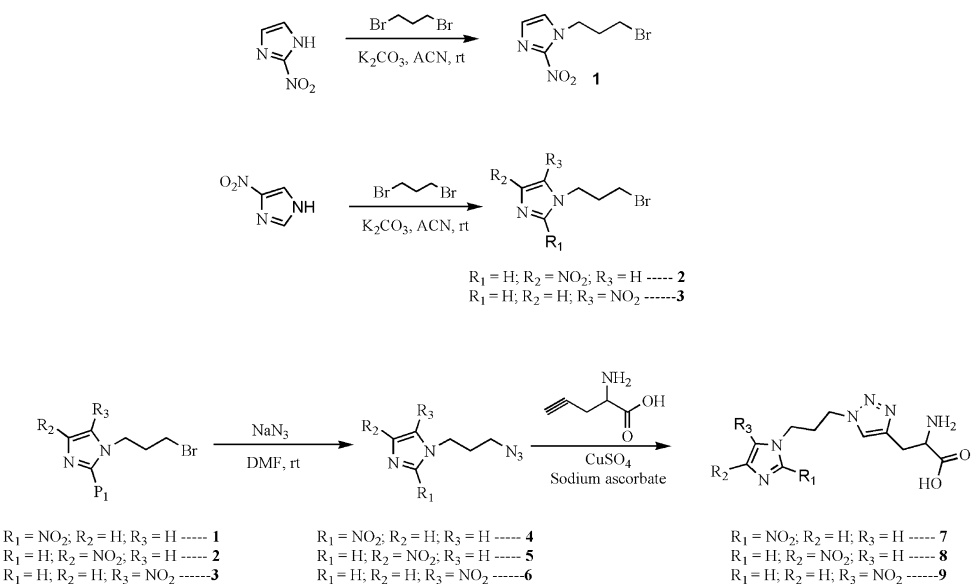

Scheme 1 Syntheses of triazole derivatives of 2-, 4- and 5-nitroimidazole

Scheme 2 Radiolabeling of 2-, 4- and 5-nitroimidazole triazole derivatives with $[^{99m}Tc(CO)_3(H_2O)_3]^+$ precursor complex

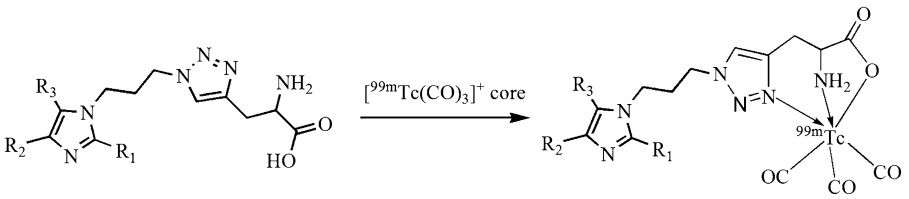

$R_1 = NO_2$; $R_2 = H$; $R_3 = H$ ----- **7**
$R_1 = H$; $R_2 = NO_2$; $R_3 = H$ ----- **8**
$R_1 = H$; $R_2 = H$; $R_3 = NO_2$ ------**9**

$R_1 = NO_2$; $R_2 = H$; $R_3 = H$ -----2-nitroimidazole complex
$R_1 = H$; $R_2 = NO_2$; $R_3 = H$ -----4-nitroimidazole complex
$R_1 = H$; $R_2 = H$; $R_3 = NO_2$ ------5-nitroimidazole complex

Table 1 Log $P_{o/w}$ values and other quality control parameters of different nitroimidazole triazole-$^{99m}Tc(CO)_3$ complexes

	Log $P_{o/w}$	Retention time in HPLC (in min)	% RCP	Specific activity (in μCi/μmol of ligand)	% Activity associated with serum proteins
$[^{99m}Tc(CO)_3(H_2O)_3]^+$ precursor complex	–	3.7 ± 0.2	–	–	–
2-Nitroimidazole triazole-$^{99m}Tc(CO)_3$ complex	−0.32 ± 0.02	20.5 ± 0.1	95.0 ± 1.00	105.55 ± 1.11	32.8 ± 1.35
4-Nitroimidazole triazole-$^{99m}Tc(CO)_3$ complex	−0.52 ± 0.01	20.0 ± 0.2	96.3 ± 0.57	107.03 ± 0.64	30.1 ± 1.06
5-Nitroimidazole triazole-$^{99m}Tc(CO)_3$ complex	−0.03 ± 0.01	21.0 ± 0.1	97.0 ± 1.00	107.77 ± 1.11	35.4 ± 0.96
4-Nitroimidazole triazole $Re(CO)_3$	–	19.5 ± 0.2	–	–	

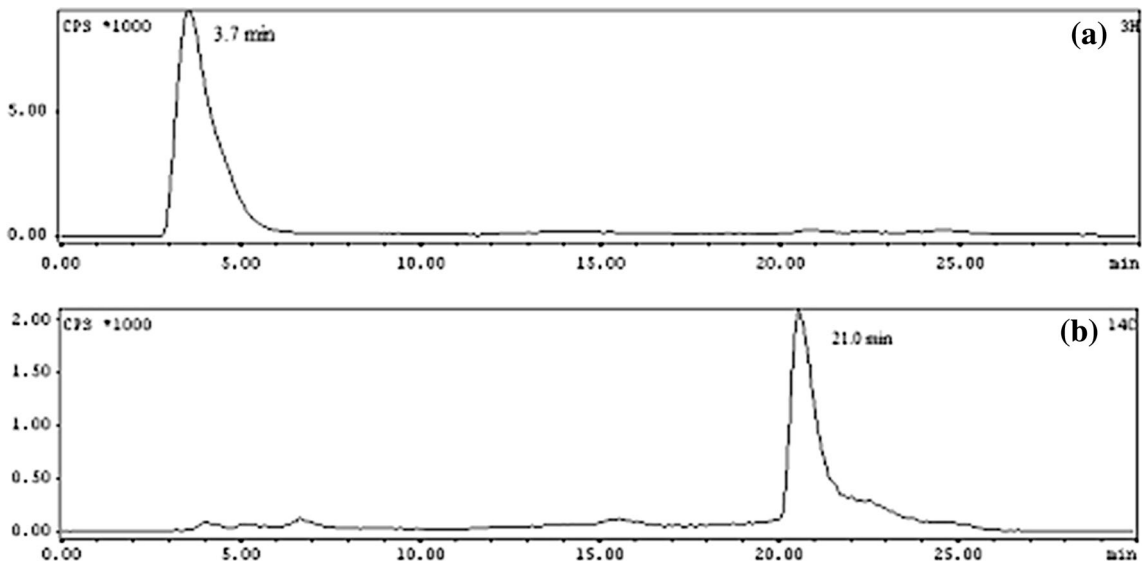

Fig. 1 HPLC elution profile of **a** $[^{99m}Tc(CO)_3(H_2O)_3]^+$ precursor complex and **b** 5-nitroimidazole triazole-$^{99m}Tc(CO)_3$ complex (**12**)

time nitroimidazole complex spends in hypoxic cells. Ease of reduction of nitroimidazole complex in hypoxic tumor cells is determined by its SERP. SERP is a molecular property which depends on the position of nitro-group in the imidazole ring. Reported SERP value of unsubstituted 2-, 4- and 5-nitroimidaozle in aqueous solution is −418, −527 and −450 mV, respectively, with respect to standard hydrogen electrode (SHE) [38]. Though modification at

N1-nitrogen of nitroimidazole ring, as done in the present work, can potentially alter the SERP values of the nitroimidazole derivative, previous studies have shown that such variations are not significant [39]. Among the different nitroimidazole triazole derivatives, we expected that 2-nitroimidazole derivative with highest SERP value will show the highest tumor uptake. However, contrary to our expectations, the 5-nitroimidazole complex showed higher tumor uptake than the 2-nitroimidazole counterpart at all the time points (Table 2). Statistical analysis showed that tumor uptake observed with 5-nitroimidazole-triazole complex is significantly higher ($p < 0.05$) than the 2-nitroimidazole counterpart at 30 and 60 min p.i. However, at 3 h p.i., the difference in tumor uptake was found to be insignificant ($p > 0.05$). Tumor uptake of 4-nitroimidazole-triazole complex was lowest among the three triazole complexes at all the time points. This is not surprising, since SERP of 4-nitroimidazole is lowest among 2-, 4- and 5-nitroimidazole. In comparison, [^{18}F]FMISO with a SERP of −389 mV (with respect to SHE) showed significantly higher uptake than any of the nitroimidazole-triazole complexes at all the time points (Table 2). It is clear from the above discussion that SERP value alone cannot explain the difference in tumor uptake between 2- and 5-nitroimidazole traizole complexes.

A possible explanation for this observation can be proposed considering the lipophilicity (Log $P_{o/w}$) (Table 1) and blood clearance of the three nitroimidazole triazole complexes (Table 2). Lipophilicity is important for smooth entry of the complex in tumor cells by passive diffusion. It could also be noted that blood clearance pattern of nitroimidazole complexes (Table 2) correlated well with their Log $P_{o/w}$ values (Table 1) and 5-nitroimidazole complex having the highest Log $P_{o/w}$ value showed the slowest blood clearance. Slow blood clearance provides more time for the radiotracer to distribute in tumor by passive diffusion. It also allows the radiotracer to spend more time in tumor cells by maintaining a positive concentration gradient between the blood pool and the tumor tissue, thus facilitating hypoxia specific reduction. We speculate that due to relatively fast blood clearance, the effective distribution and time spent by 2-nitroimidazole complex in tumor may be lower compared to the 5-nitroimidazole counterpart. This could have resulted in lower tumor uptake of the former despite having a better SERP. Blood clearance of 4-nitroimidazole complex was fastest among the three triazole complexes (Table 2) and combined with the low SERP value, this complex showed the lowest tumor uptake among the three nitroimidazole triazole complexes evaluated.

On the other hand, at 30 min p.i., activity of [^{18}F]FMISO in blood was higher than any other nitroimidazole-triazole complex (Table 2). This must have facilitated better diffusion (Log $P_{o/w}$ of [^{18}F]FMISO –0.41 [10]) and distribution of [^{18}F]FMISO in tumor compared to other nitroimidazole complexes. A careful look at the blood clearance pattern (Table 2) will reveal that blood clearance of [^{18}F]FMISO was the slowest among the four nitroimidazole radiotracers till 1 h p.i. Consequently, [^{18}F]FMISO could be anticipated to spend more time in tumor cells than any other nitroimidazole-triazole complex. All these favorable factors resulted in higher tumor uptake by [^{18}F]FMISO.

It is worth mentioning here that a metronidazole triazole-^{99m}Tc(CO)$_3$ complex, similar to the 5-nitroimidazole-triazole-^{99m}Tc(CO)$_3$ complex evaluated herein, has been reported [27]. The difference between the two complexes is in the linker used to couple the nitroimidazole and the triazole moiety. The metronidazole triazole-^{99m}Tc(CO)$_3$ complex, reported earlier, was less lipophilic than the 5-nitroimidazole triazole-^{99m}Tc (CO)$_3$ complex evaluated in the present study. Its clearance from blood was faster and tumor uptake lower when compared to 5-nitroimidazole triazole-^{99m}Tc(CO)$_3$ complex (**12**). This is similar to the observations made in the present study, where complexes with faster blood clearance show lower tumor uptake.

Table 2 Activity of different nitroimidazole-triazole-^{99m}Tc(CO)$_3$ complexes and [^{18}F]FMISO observed in tumor and blood at different time points ($n = 5$)

		^{99m}Tc(CO)$_3$ complex			[^{18}F]FMISO[b]
		2-Nitroimidazole-triazole	4-Nitroimidazole-triazole	5-Nitroimidazole-triazole	
Tumor %ID/g (s.d)[a]	30 min	1.41 ± 0.08	0.63 ± 0.09	2.03 ± 0.32	4.65 ± 0.86
	60 min	0.97 ± 0.06	0.56 ± 0.05	1.45 ± 0.08	3.70 ± 0.09
	180 min	0.75 ± 0.14	0.26 ± 0.02	0.81 ± 0.06	2.04 ± 0.14
Blood %ID/g (s.d)[a]	30 min	0.95 ± 0.05	0.73 ± 0.08	1.91 ± 0.14	3.95 ± 0.31
	60 min	0.62 ± 0.12	0.37 ± 0.02	1.31 ± 0.11	2.38 ± 0.42
	180 min	0.43 ± 0.06	0.35 ± 0.04	0.77 ± 0.04	0.53 ± 0.07

[a] *%ID/g* percentage injected dose per gram, *SD* standard deviation

[b] Ref. [26]

Table 3 Biodistribution of various nitroimidazole triazole-$^{99m}Tc(CO)_3$ complexes (**10**, **11** & **12**) (%ID/gram) in Swiss mice bearing fibrosarcoma tumor ($n = 5$) at three different time points

Organ	2-Nitroimidazole complex			4-Nitroimidazole complex			5-Nitroimidazole complex		
	30 min	1 h	3 h	30 min	1 h	3 h	30 min	1 h	3 h
Lung	1.55 ± 0.38	0.99 ± 0.04	0.77 ± 0.04	1.18 ± 0.20	0.68 ± 0.10	0.47 ± 0.07	2.09 ± 0.27	1.48 ± 0.19	0.84 ± 0.20
Heart	1.42 ± 0.19	0.84 ± 0.01	0.57 ± 0.01	0.56 ± 0.03	0.41 ± 0.02	0.21 ± 0.03	0.74 ± 0.06	0.65 ± 0.03	0.51 ± 0.02
Intestine	9.32 ± 0.97	10.29 ± 0.89	10.54 ± 2.33	19.64 ± 2.97	21.19 ± 0.80	21.78 ± 1.21	6.42 ± 1.24	9.06 ± 0.26	8.72 ± 0.64
Liver	8.79 ± 0.38	6.81 ± 0.99	5.29 ± 1.15	8.51 ± 0.73	5.68 ± 1.12	3.65 ± 0.40	11.62 ± 1.00	7.96 ± 0.34	6.29 ± 0.41
Spleen	0.70 ± 0.04	0.58 ± 0.13	0.49 ± 0.07	0.66 ± 0.07	0.64 ± 0.12	0.19 ± 0.05	0.58 ± 0.11	1.33 ± 0.13	0.35 ± 0.05
Kidney	4.69 ± 0.52	2.77 ± 0.40	2.35 ± 0.38	2.41 ± 0.23	1.09 ± 0.10	0.87 ± 0.06	8.47 ± 1.12	6.64 ± 0.72	4.67 ± 0.26
Muscle	0.48 ± 0.08	0.37 ± 0.03	0.33 ± 0.03	0.36 ± 0.04	0.18 ± 0.01	0.10 ± 0.01	0.25 ± 0.02	0.37 ± 0.03	0.15 ± 0.01
T/B[a]	1.48 ± 0.13	1.59 ± 0.35	1.80 ± 0.50	0.87 ± 0.19	1.53 ± 0.15	0.78 ± 0.14	1.06 ± 0.16	1.11 ± 0.13	1.05 ± 0.03
T/M[a]	2.99 ± 0.50	2.59 ± 0.27	2.33 ± 0.60	1.78 ± 0.43	3.20 ± 0.22	2.56 ± 0.38	8.15 ± 1.42	3.92 ± 0.23	5.39 ± 0.53

[a] *T/B* tumor to blood ratio, *T/M* tumor to muscle ratio

Table 3 shows the distribution of nitroimidazole-triazole complexes in other organs at different time points. It could be noted that major clearance of activity of all the complexes is through hepatobiliary route, indicated by presence of significant level of activity in liver and gastrointestinal tract. Activity observed in other vital organs like lung, heart, spleen and kidney gradually cleared with time.

The tumor to blood and tumor to muscle ratio obtained with the three nitroimidazole complexes are also shown in Table 3. All the three nitroimidazole complexes showed tumor to blood ratio ranging from 1 to 1.8 and tumor to muscle ratio between 2 and 5.

Conclusions

Present study reports an unexpected result wherein a 5-nitroimidazole-$^{99m}Tc(CO)_3$ complex showed better tumor uptake than the 2-nitroimidazole counterpart. A possible reason for this observation was attributed to the slower blood clearance of the radiotracer. Present study also highlights the necessity of evaluating nitroimidazole complexes other than 2-nitroimidazole in order to exclude the possibility of overlooking potential nitroimidazole radiotracers other than 2-nitroimidazole for hypoxia detecting applications.

Acknowledgments Authors acknowledge all concerned staff of Radiochemicals and Radiation Sources Section, Isotope Production and Application Division, BARC, for providing Molybednum-99 isotope.

Conflict of interest The authors clarify that there is no financial or other conflict of interests in the work reported.

References

1. Mees G, Dierckx R, Vangestel C, Van de Wiele C (2009) Molecular imaging of hypoxia with radiolabelled agents. Eur J Nucl Med Mol Imaging 36:1674–1686
2. Gray LH, Conger AD, Ebert MB (1953) The concentration of oxygen dissolved in tissues at the time of irradiation as a factor in radiotherapy. J Radiol 26:638–648
3. Höckel M, Schlenger K, Aral B, Mitze M, Schäffer U, Vaupel P (1996) Association between tumor hypoxia and malignant progression. Cancer Res 56:4509–4515
4. Fyles AW, Milosevic M, Wong R, Kavanagh MC, Pintilie M, Sun A, Chapman W, Levin W, Manchul L, Keane TJ, Hill RP (1998) Oxygenation predicts radiation response and survival in patients with cervix cancer. Radiother Oncol 48:149–156
5. Nordsmark M, Overgaard M, Overgaard J (1996) Pretreatment oxygenation predicts radiation response in advanced squamous cell carcinoma of the head and neck. J Radiother Oncol 41:31–39
6. Brizel DM, Sibley GS, Prosnitz LR, Scher RL, Dewhirst MW (1997) Tumor hypoxia adversely affects the prognosis of carcinoma of the head and neck. J Radiat Oncol Biol Phys 38:285–289

7. Nordsmark M, Bentzen SM, Rudat V, Brizel D, Lartigau E, Stadler P, Becker A, Adam M, Molls M, Dunst J, Terris DJ, Overgaard J (2005) Prognostic value of tumor oxygenation in 397 head and neck tumors after primary radiation therapy. An international multi-center study. J Radiother Oncol 77:18–24
8. Duffy JP, Eibl G, Reber HA, Hines OJ (2003) Influence of hypoxia and neoangiogenesis on the growth of pancreatic cancer. J Mol Cancer 2:12
9. Brizel DM, Scully SP, Harrelson JM, Layfield LJ, Bean JM, Prosnitz LR, Dewhirst MW (1996) Tumor oxygenation predicts for the likelihood of distant metastases in human soft tissue sarcoma. Cancer Res 56:941–943
10. Krohn KA, Link JM, Mason RP (2008) Molecular imaging of hypoxia. J Nucl Med 2(Suppl):129S–148S
11. Sorger D, Patt M, Kumar P, Wiebe LI, Barthel H, Seese A, Dannenberg C, Tannapfel A, Kluge R, Sabri O (2003) [^{18}F]Fluoroazomycinarabinofuranoside (18FAZA) and [^{18}F]fluoromisonidazole (18FMISO): a comparative study of their selective uptake in hypoxic cells and PET imaging in experimental rat tumors. Nucl Med Biol 30:17–26
12. Komar G, Seppänen M, Eskola O, Lindholm P, Grönroos TJ, Forsback S, Sipilä H, Evans SM, Solin O, Minn H (2008) ^{18}F-EF5: a new PET tracer for imaging hypoxia in head and neck cancer. J Nucl Med 49:1944–1951
13. Rasey JS, Hofstrand PD, Chin LK, Tewson TJ (1999) Characterization of [^{18}F]fluoroetanidazole, a new radiopharmaceutical for detecting tumor hypoxia. J Nucl Med 40:1072–1079
14. Lewis JS, McCarthy DW, McCarthy TJ, Fujibayashi Y, Welch MJ (1999) Evaluation of 64Cu-ATSM in vitro and in vivo in a hypoxic tumor model. J Nucl Med 40:177–183
15. Bonnitcha PD, Bayly SR, Theobald MB, Betts HM, Lewis JS, Dilworth JR (2010) Nitroimidazole conjugates of bis(thiosemicarbazonato)^{64}Cu(II)—potential combination agents for the PET imaging of hypoxia. J Inorg Biochem 104:126–135
16. Grunbaum Z, Freauff SJ, Krohn KA, Wilbur DS, Magee S, Rasey JS (1987) Synthesis and characterization of congeners of misonidazole for imaging hypoxia. J Nucl Med 28:68–75
17. Evans SM, Kachur AV, Shiue CY, Hustinx R, Jenkins WT, Shive GG, Karp JS, Alavi A, Lord EM, Dolbier WR Jr, Koch CJ (2000) Noninvasive detection of tumor hypoxia using the 2-nitroimidazole [^{18}F]EF1. J Nucl Med 41:327–336
18. Zha Z, Zhu L, Liu Y, Du F, Gan H, Qiao J, Kung HF (2011) Synthesis and evaluation of two novel 2-nitroimidazole derivatives as potential PET radioligands for tumor imaging. Nucl Med Biol 38:501–508
19. Tatum JL, Kelloff GJ, Gillies RJ, Arbeit JM, Brown JM, Chao KS, Chapman JD, Eckelman WC, Fyles AW, Giaccia AJ, Hill RP, Koch CJ, Krishna MC, Krohn KA, Lewis JS, Mason RP, Melillo G, Padhani AR, Powis G, Rajendran JG, Reba Robinson SP, Semenza GL, Swartz HM, Vaupel P, Yang D, Croft B, Hoffman J, Liu G, Stone H, Sullivan D (2006) Hypoxia: importance in tumor biology, noninvasive measurement by imaging, and value of its measurement in the management of cancer therapy. Int J Radiat Biol 82:699–757
20. Ballinger JR (2001) Imaging hypoxia in tumors. Semin Nucl Med 31:321–329
21. Nunn A, Linder K, Strauss HW (1995) Nitroimidazoles and imaging hypoxia. Eur J Nucl Med 22:265–280
22. Mallia MB, Subramanian S, Mathur A, Sarma HD, Venkatesh M, Banerjee S (2010) Synthesis and evaluation of 2-, 4-,5-substituted nitroimidazole-iminodiacetic acid-^{99m}Tc(CO)$_3$ complexes to target hypoxic tumors. J Label Compd Radiopharm 53:535–542
23. Mallia MB, Kumar C, Mathur A, Sarma HD, Banerjee S (2012) On the structural modification of 2-nitroimidazole-^{99m}Tc(CO)$_3$ complex, a hypoxia marker, for improving in vivo pharmacokinetics. Nucl Med Biol 39:1236–1242
24. Mallia MB, Subramanian S, Mathur A, Sarma HD, Venkatesh M, Banerjee S (2008) On the isolation and evaluation of a novel unsubstituted 5-nitroimidazole derivative as an agent to target tumor hypoxia. Bioorg Med Chem Lett 18:5233–5237
25. Mallia MB, Subramanian S, Mathur A, Sarma HD, Venkatesh M, Banerjee S (2008) Comparing hypoxia-targeting potential of ^{99m}Tc(CO)$_3$-labeled 2-nitro and 4-nitroimidazole. J Label Compd Radiopharm 51:308–313
26. Mallia MB, Subramanian S, Mathur A, Sarma HD, Banerjee S (2014) A study on nitroimidazole-^{99m}Tc(CO)$_3$ complexes as hypoxia marker: some observations towards possible improvement in vivo efficacy. Nucl Med Biol 41:600–610
27. Fernández S, Giglio J, Rey AM, Cerecetto H (2012) Influence of ligand denticity on the properties of novel ^{99m}Tc(I)–carbonyl complexes. Application to the development of radiopharmaceuticals for imaging hypoxic tissue. Bioorg Med Chem 20:4040–4048
28. Giglio J, Dematteis S, Fernández S, Cerecetto H, Rey AM (2014) Synthesis and evaluation of a new ^{99m}Tc(I)-tricarbonyl complex bearing the 5-nitroimidazol-1-yl moiety as potential hypoxia imaging agent. J Label Compd Radiopharm 57:403–409
29. Lee ST, Scott AM (2007) Hypoxia positron emission tomography imaging with ^{18}F-fluoro misonidazole. Semin Nucl Med 37:451–461
30. Hoebers FJP, Janssen HLK, Olmos RAV, Sprong D, Nunn AD, Balm AJ, Hoefnagel CA, Begg AC, Haustermans KM (2002) Phase 1 study to identify tumour hypoxia in patients with head and neck cancer using ^{99m}Tc BRU 59-21. Eur J Nucl Med Mol Imaging 29:1206–1211
31. Alberto R, Schibli R, Schubiger PA, Abram U, Kaden TA (1996) Reactions with the technetium and rhenium carbonyl complexes $(NEt_4)_2[MX_3(CO)_3]$. Synthesis and structure of $[Tc(CN\text{-}Bu^t)_3(CO)_3$ and (NEt_4) $[Tc_2(\mu\text{-}SCH_2CH_2OH)_3(CO)_6]$. Polyhedron 15:1079–1089
32. Mindt TL, Müller C, Melis M, de Jong M, Schibli R (2008) Click-to-chelate: in vitro and in vivo comparison of a ^{99m}Tc(CO)$_3$-labeled N(tau)-histidine folate derivative with its isostructural, clicked 1,2,3-triazole analogue. Bioconjug Chem 19:1689–1695
33. Rostovtsev VV, Green LG, Fokin VV, Sharpless KB (2002) A stepwise huisgen cycloaddition process: copper(I)-catalyzed regioselective "ligation" of azides and terminal alkynes. Angew Chem 41:2596–2599
34. Bock VD, Hiemstra H, Van Maarseveen JH (2006) CuI-catalyzed alkyne-azide "click" cycloadditions from a mechanistic and synthetic perspective. Eur J Org Chem 2006:51–68
35. Alberto R, Schibli R, Egli A, Schubiger AP (1998) A novel organometallic aqua complex of technetium for the labeling of biomolecules:synthesis of $[^{99m}Tc(H_2O)_3(CO)_3]^+$ from $[^{99m}TcO_4]^-$ in aqueous solution and its reaction with a bifunctional ligand. J Am Chem Soc 120:7987–7988
36. Troutner DE, Volkert WA, Hoffman TJ, Holmes RA (1984) A neutral lipophilic complex of ^{99m}Tc with a multidentate amine oxime. Int J Appl Radiat Isot 35(6):467–470
37. Adams MF, Dorie MJ, Brown JM (1999) Oxygen tension measurements of tumors growing in mice. Int J Radiat Oncol Biol Phys 45:171–180
38. Wardman P (1989) Reduction potentials of one electron couples involving free radicals in aqueous solutions. J Phys Chem 18:1637–1755
39. Adams GE, Cooke MS (1969) Electron-affinic sensitization. I. A structural basis for chemical radiosensitizers in bacteria. Int J Radiat Biol Relat Stud Phys Chem Med 15:457–471